Quantifying electron-phonon coupling in $CdTe_{1-x}Se_x$ nanocrystals via coherent phonon manipulation

B. T. Spann and X. Xu[a)]
School of Mechanical Engineering and Birck Nanotechnology Center, Purdue University, West Lafayette, Indiana 47907, USA

(Received 15 July 2014; accepted 15 August 2014; published online 26 August 2014)

We employ ultrafast transient absorption spectroscopy with temporal pulse shaping to manipulate coherent phonon excitation and quantify the strength of electron-phonon coupling in $CdTe_{1-x}Se_x$ nanocrystals (NCs). Raman active CdSe and CdTe longitudinal optical phonon (LO) modes are excited and probed in the time domain. By temporally controlling pump pulse pairs to coherently excite and cancel coherent phonons in the $CdTe_{1-x}Se_x$ NCs, we estimate the relative amount of optical energy that is coupled to the coherent CdSe LO mode. © *2014 AIP Publishing LLC*.
[http://dx.doi.org/10.1063/1.4894176]

Understanding light-matter interactions in semiconducting nanocrystals has been at the forefront of modern condensed matter physics and physical chemistry for several decades. Much of the interest in semiconducting nanocrystals (NCs) has been driven by the tunable quantum confinement that is possible through various means of chemical synthesis. Controllable quantum confinement provides a means of electronic energy level engineering and has made semiconducting NCs a tool for conquering various scientific and engineering challenges. Third generation photovoltaic (PV) technology is one of the areas where NCs have been employed to take advantage of confinement enhanced phenomena such as multi-exciton generation (MEG) and hot-electron transfer. MEG aims to increase the photocurrent of a solar cell and has been shown to be possible in various lead chalcogenides.[1–4] Hot-electron solar cells, on the other hand, aim to increase the photovoltage of the solar cell by extracting hot-electrons prior to thermalizing to the band-edge. Semiconductor NCs have discrete energy level spacing on the order of hundreds of meV requiring more time consuming multiphonon emission, commonly referred to as the phonon bottleneck as described by Nozik.[5] The theoretical increased intraband relaxation time should enhance the potential to extract the hot-carriers, although evidence for hot-electron transfer has been more difficult to come by with only a few convincing works in the literature to relay its potential.[6–9]

A common material for hot-carrier type cells is CdSe because its bandgap energy can be tuned within the visible spectrum. A drawback to CdSe, however, is that there is a competing relaxation pathway to the phonon bottleneck known as Auger-like thermalization and is shown in the seminal works by Brus,[10] Efros *et al.*,[11] and Klimov.[12,13] Auger-like thermalization causes intraband relaxation times of hot-excitons to be on the order of ~1 ps for CdSe quantum dots as a result of electrons scattering with holes and subsequently holes emitting phonons and relaxing to the band-edge.[11,12,14–16] Therefore, it is important to investigate the details of charge carriers coupling to phonons in these materials. While the ultrafast electronic relaxation has been well characterized, e.g., by the above mentioned studies, fewer have attempted to elucidate ultrafast phonon dynamics in NCs. Initial works by Machol *et al.*[17] and Bragas *et al.*[18,19] and more recently Sagar *et al.*[20] and Chai *et al.*[21] have observed and made attempts to quantify ultrafast optically generated coherent phonons in NCs. However, none has attempted to directly measure/quantify the efficiency of charge carrier phonon coupling. Quantifying the amount of photon energy coupled to the various phonon modes is vital to gauge NCs for hot-carrier PV applications.

Ultrafast pump-probe spectroscopy can provide a means to examine phonon vibrations in the time domain. The mechanism responsible for generating the vibrational coherences observed in pump-probe experiments is generalized as impulsive stimulated Raman scattering (ISRS). A special case of ISRS is the displacive excitation of coherent phonons (DECP) mechanism which excites the A_1 symmetric Raman modes.[22–24] In some of our previous works, we have developed methods of quantitatively analyzing the lattice dynamics in materials. Specifically, we have employed transient reflectance spectroscopy with temporal pulse shaping to assess the electron-phonon coupling strength in bulk bismuth.[25] In this work, we aim to quantify the electron-phonon coupling in the photo-excited NCs by means of transient absorption spectroscopy and temporal pulse shaping. Specifically, we excite coherent optical phonons in the NCs and evaluate the resulting quasi-equilibrium lattice temperature. By enhancing and canceling coherent lattice vibrations using temporally shaped ultrafast pulses, the relative percentage of energy coupled from the excited electrons to phonon modes is quantified. Through understanding the photon-electron-phonon energy conversion processes in semiconducting NCs, attempts at minimizing the unwanted thermalization loss can be made by altering the NC size, shape, and composition.

The $CdTe_{1-x}Se_x$ NCs are embedded in 3 mm thick borosilicate glass matrix alloyed with $x = 0.32$ of Se (RG780 light filter from Schott Glass, Inc.). For $x < 0.36$, the $CdTe_{1-x}Se_x$ NCs are in the zincblende cubic structure.[19,26] The embedded NCs' average radii are ~3.9 nm with size distribution within ~10% of its nominal value.[18,19,21] The linear absorption spectrum was measured using a Perkin Elmer Lambda 950 UV/

a)Author to whom correspondence should be addressed. Electronic mail: xxu@purdue.edu.

Vis spectrophotometer and is depicted in Fig. 1. As shown in Fig. 1(a), the first excitonic transition occurs at photon wavelengths of approximately 740 nm (1.68 eV), which matches with previously reported values.[18,19,21] The Raman spectrum of the $CdTe_{1-x}Se_x$ sample was gathered using a Horiba LabRAM Raman spectrometer and is shown in Fig. 1(b), which reveals longitudinal optical (LO) peaks of both CdTe ($\sim$160 cm^{-1}) and CdSe ($\sim$200 cm^{-1}) and their overtone modes (2LO: 340–400 cm^{-1}).[18,19,21] The peak near $\sim$260 cm^{-1} is expected to be a mixed transverse optical (TO) and LO modes.[18]

Degenerate ultrafast pump-probe experiments were performed to collect transient absorption (TA) data for the sample. The TA experiment consists of a Ti:sapphire femtosecond pulse amplifier that produces sub 30 fs pulses at 800 nm with a repetition rate of 5 kHz. The pump beam is sent through a temporal pulse shaper (Biophotonics Solutions) and then through a mechanical chopper rotating at 500 Hz. The pump and probe beams are focused on the sample non-colinearly at an angle of $\sim$180 mrad to $1/e^2$ spot diameters of 400 μm and 100 μm, respectively. See our other works for more details of the pump-probe setup.[16] Both pump and probe wavelengths were set to 800 nm and were perpendicularly polarized with respect to each other. The pump and probe wavelengths are located on the rising edge of the linear absorption spectra as depicted by the vertical arrow in Fig. 1(a). The resultant fluence dependent TA data are shown in Fig. 2(a). As can be seen, the TA data show a rapid increase in the absorption followed by decay to a non-zero positive value within the first $\sim$5 ps. The positive TA signal is the result of two potential photophysical events. The first is through the carrier induced Stark effect (CISE). The CISE is possible for the current experiment because the pump beam has a bandwidth of $\sim$40 nm; therefore, when the pump photons are absorbed, the consequential exciton generation creates a static electric field causing the band-gap energy to become reduced,[12,14–16] thus more probe photons can be absorbed. The second route to a positive TA signal is via intraband absorption, i.e., when the pump photon is absorbed and the electron hole pair is generated, the electrons in the conduction band are then allowed to absorb the probe photon to be pumped higher into the conduction band.[21]

Once the pump and probe photons are absorbed by the sample, the excitons can then couple their energy to LO phonons then to acoustic phonons, subsequently heating the lattice. The TA signals portray coherent LO phonon generation as shown by the oscillatory component in Fig. 2(a). In order to analyze the frequency response of the TA signals, a second order Butterworth filter with Gaussian sampling was applied to remove the background electronic signal and the Fast Fourier transform (FFT) was calculated. The FFT spectra in Fig. 2(b) display the same LO mode peaks from the CdTe ($\sim$160 cm^{-1}) and CdSe ($\sim$200 cm^{-1}) as the Raman data in Fig. 1(b). The dephasing time of the coherent LO modes is about 2 ps, which is the time period for the LO-to-acoustic phonon down version. This is consistent with the time resolved Raman data gathered by Hannah *et al.*,[27]

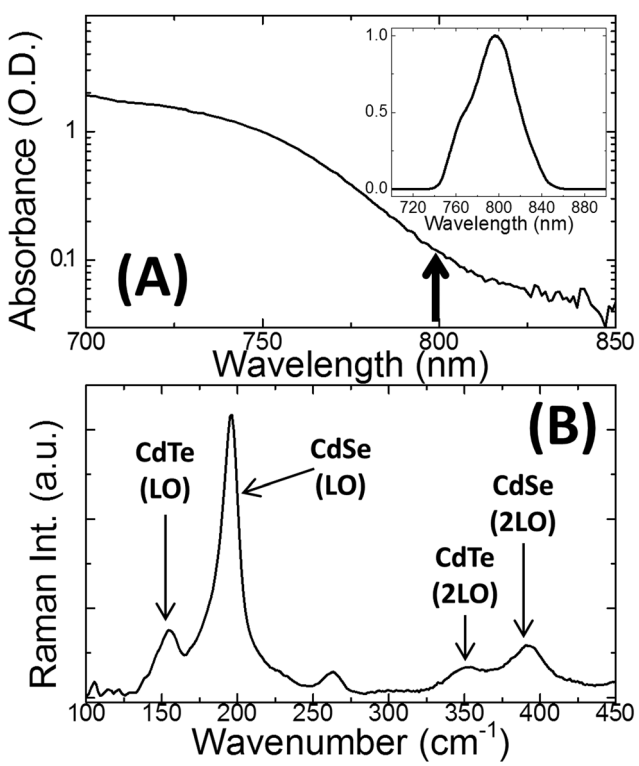

FIG. 1. (a) Linear absorption spectrum of the $CdTe_{1-x}Se_x$ NCs with pump and probe wavelength noted (vertical arrow) for transient absorption studies and pump/probe spectrum shown in the inset. (b) The Raman spectrum.

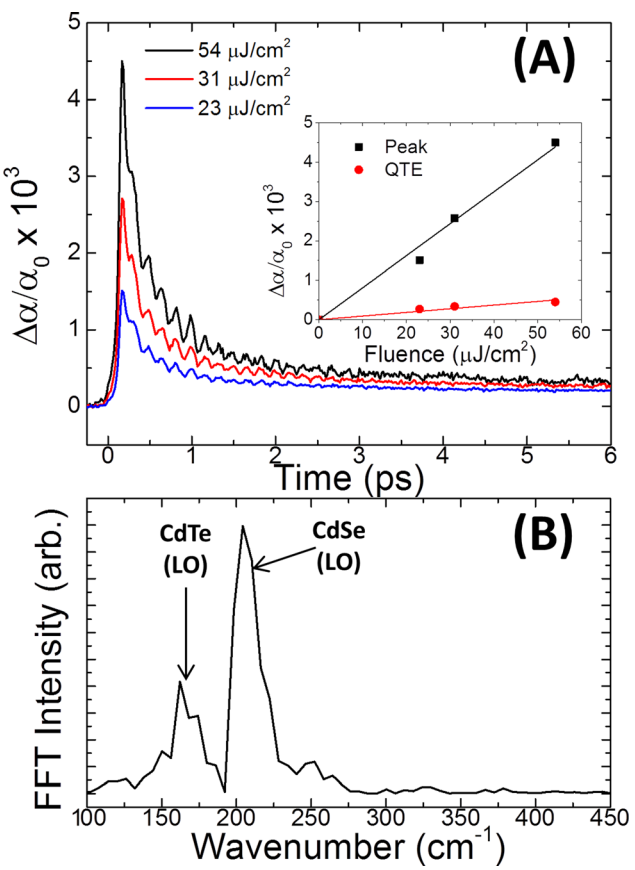

FIG. 2. (a) Degenerate transient absorption measurements (with pump perpendicularly polarized to the probe) of the $CdTe_{1-x}Se_x$ NCs with varying fluence and inset providing a double-y scale plot of peak values and QTE values of the TA trends. (b) Fast Fourier transform calculation results of the 54 $\mu J/cm^2$ transient absorption case.

who observed LO-to-acoustic down-conversion on a time scale of 2 ps for CdSe quantum dots.

The inset of Fig. 2(a) shows a plot for the fluence dependent peak and quasi-thermal equilibrium (QTE) $\Delta\alpha/\alpha_0$ values. The QTE values were taken at ~2.5 ps. Both plots in the inset show approximately linear trends. The linear trend in peak values suggests that there is an approximate monotonic increase in non-equilibrium charge carriers excited as the pump fluence is increased within the fluence range used here. After the excitation of the charge carriers, electron-phonon scattering processes cause the charge-carriers to relax into QTE. Given the timescale under consideration, the thermal energy stored in the NCs is not able to diffuse into the surrounding medium, thus we observe a nonzero $\Delta\alpha/\alpha_0$ value. Additionally, we also observe a linear trend in QTE value that suggests that there is also a monotonic increase in QTE with the pump fluence. Electron-electron, electron-phonon, and electron-hole scattering are, in general, non-linear processes; however, given the low fluence range used here, the ratio between the two linear trends is constant, suggesting that the scattering rates at these fluences are similar.

To estimate the percentage of energy coupled into the NC lattice through the LO mode, we employ a temporal pulse shaper to generate double pulses and delicately control the pulse-to-pulse delay and energy of each pulse. The second pulse of the double pulse pairs was controlled to be at 1 T and 1.5 T, where T is the period of CdSe LO mode oscillation (i.e., T = 166.7 fs from Fig. 2(b)) for enhancing (E) and canceling (C) coherent phonon oscillations, respectively. From Fig. 2(b), it is seen that there are two dominant LO modes observed. Using double pulse pairs, we can only enhance or cancel one of the two modes, and here we choose the LO mode for CdSe as it is the stronger of the two. The results of using the double pulse pairs with respective cross-correlations are shown in Fig. 3(a). Also shown in Fig. 3(a) is the single pulse experiment; all cases underwent the same total input fluence of 54 μJ/cm^2. As illustrated in Fig. 3(a), the single pulse case and the enhancement case come to a nearly the same QTE $\Delta\alpha/\alpha_0$ value (at ~2.5 ps), while the cancelation case shows a lower $\Delta\alpha/\alpha_0$ value. Furthermore, by using the appropriate ratio of the second pulse to the first pulse energy (0.9:1), nearly complete oscillation cancellation was achieved.

The difference in the QTE $\Delta\alpha/\alpha_0$ values for the optical phonon enhancement and cancellation allows for the determination of the amount of energy coupled into optical phonons. In order to show this difference more clearly, the difference between the enhanced and cancelled TA signals in Fig. 3(a) is plotted in Fig. 3(b), which shows the difference in QTE value as well as the difference in the rate of thermalization of the excited carriers. The positive values for the difference of $(\Delta\alpha - \Delta\alpha_C)/\alpha_0$, 1.8×10^{-4}, and 1.4×10^{-4} at QTE for the single pulse and enhancement cases, respectively, indicate that the lattice temperature of phonon cancelation case is lower. This is verified from Fig. 3(c) which depicts the temperature dependent absorbance of the light at probe wavelength measured under steady-state conditions. This temperature dependent absorption is consistent with the Varshni-like temperature dependent behavior of the band-gap energy in CdSe NCs.[28] The temperature dependent absorbance data were fitted to an empirical Varshni-form equation defined by $\alpha/\alpha_0 = A + BT^2/(C+T)$, with the fitted parameters A = 0.97, B = 0.04 °C^{-1}, and C = 771.70 °C. The increase in absorbance of the 800 nm light is a result of temperature dependent dilation of the lattice and a shift in the relative energies of the valence and conduction bands from increased electron-phonon scattering.[29]

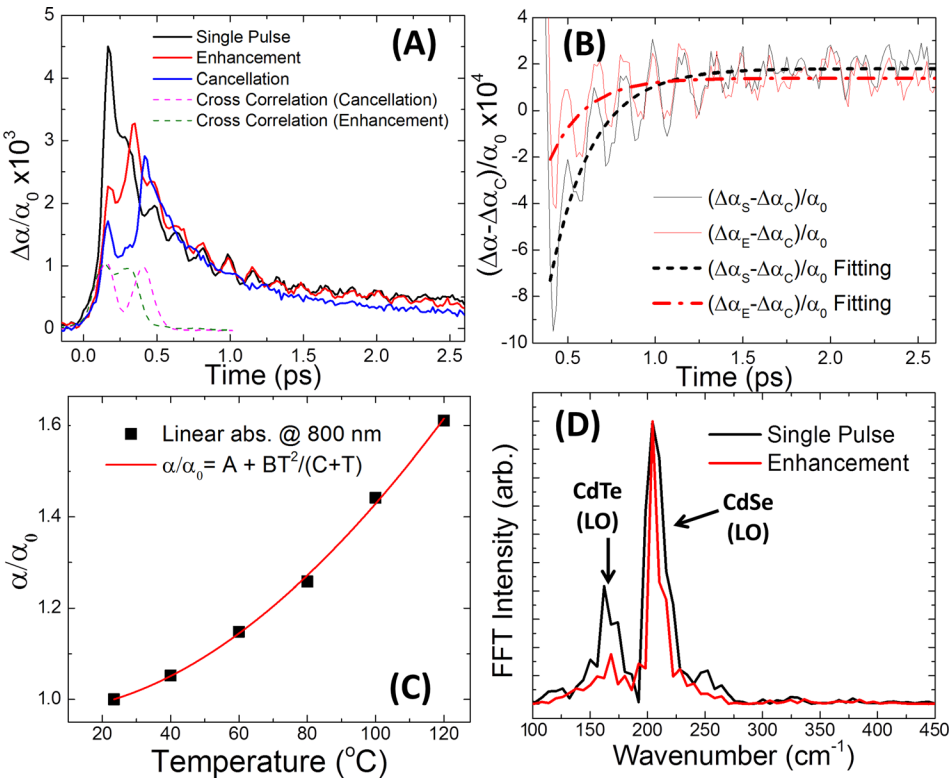

FIG. 3. (a) Single and double pulse transient absorption traces with constant total pump fluence of 54 μJ/cm^2. The second pulses for the double pulses cases arrive at 166.7 fs and 250.0 fs after initial excitation pulses for enhancement and cancelation, respectively. Also shown are the respective cross-correlation traces for the double pulse cases. (b) Difference between single pulse and cancellation as well as enhancement and cancellation cases with background exponential fittings for each. (c) Temperature dependent absorbance taken at the 800 nm probe wavelength. (d) Comparison of the normalized FFT data for the single pulse and enhancement cases.

The higher lattice temperature when the coherent optical phonons are present can be understood in terms of the energy relaxation pathways in NCs. When the optical phonon modes are suppressed (cancelled), the efficient energy relaxation pathway from LO to acoustic mode down conversion is impaired, resulting in a lower lattice temperature that is associated with the less efficient direct coupling between excitons and acoustic phonons. Furthermore, we observe a slightly higher QTE value for the single pulse case when compared with the other two cases. The reason the single pulse case results in the higher lattice temperature when compared to the enhancement case is likely due to imperfect enhancement as well as partial cancellation of the CdTe LO mode in the enhancement case. The partial cancelation of the CdTe LO mode is evident when comparing the FFT data for the single pulse and enhancement cases, which is shown in Fig. 3(d). Figure 3(d) shows a reduced relative intensity of the CdTe LO mode as well as a slightly sharper CdSe LO mode peak, both of which would reduce the potential of scattering when compared with the single pulse case. For the single pulse case, the full width half maximum (FWHM) of the CdSe LO mode is nearly double that of the enhancement case, thus providing a broader spectrum of phonon modes through which the electrons can scatter.

In order to compute the relative contribution to lattice heating from the electron-optical phonon coupling, we start by calculating the energy required for a temperature increase in the lattice ($\Delta Q''$), which can be estimated as $\Delta Q'' = \rho t f C_p \Delta\alpha (d\alpha/dT)^{-1}$, where $\rho = 6.08 \times 10^{-3}$ kg/cm^3,[30] $t = 0.3$ cm, $f = 0.075$,[18] and $C_p = 225.6$ mJ/kg/K[30] are the weighted density of the $CdTe_{1-x}Se_x$, thickness of the sample, filling factor of the $CdTe_{1-x}Se_x$ NCs in the glass matrix, and the weighted specific heat of $CdTe_{1-x}Se_x$, respectively. In QTE at approximately 2.5 ps, Fig. 3(b) shows that $\Delta\alpha/\alpha_0 = 1.8 \times 10^{-4}$ and 1.4×10^{-4} at QTE for the single pulse and enhancement cases, respectively. For $d\alpha/dT$, we can find the derivative of the Varshni equation we used to fit the temperature dependent absorption data in Fig. 3(c), i.e., $d\alpha/dT = (BT(2C+T)/(C+T)^2)\alpha_0$. Substituting the fitted parameters mentioned above and evaluating the expression at the experimental condition of 23 °C, we find that $d\alpha/dT = 2.28 \times 10^{-3}$ K^{-1}. Substituting these values into the expression for energy difference, we find that $\Delta Q'' = 2.43\,\mu$J/cm^2 and $1.89\,\mu$J/cm^2. Using $(\int P(\lambda)\tau(\lambda)d\lambda)/(\int P(\lambda)d\lambda)$, where $P(\lambda)$ and $\tau(\lambda)$ are the pump spectrum and transmission spectrum of the $CdTe_{1-x}Se_x$ NC sample, we found that ~43% of the pump fluence was absorbed to generate energy carriers. Therefore, the total energy coupled to the CdSe LO phonon constitutes ~10.5% (=2.43/(54 × 0.43)) and ~8.2% of the absorbed photon energy for the single pulse and enhancement cases. As mentioned above, the discrepancy in the two values is likely due to imperfect phonon enhancement as well as partial cancelation of the CdTe LO phonon mode.

To conclude, we have shown a technique for quantifying the strength of electron-coherent phonon coupling in $CdTe_{1-x}Se_x$ NCs using ultrafast TA spectroscopy. Raman active CdSe and CdTe LO modes are observed in the TA experiments. Using temporal pulse shaping to coherently excite and cancel the coherent phonons in the $CdTe_{1-x}Se_x$ NCs, we were able to estimate the relative amount of input optical energy that is coupled to the coherent CdSe LO mode through the photo-excited carriers.

Support for this work has been provided by the National Science Foundation and is gratefully acknowledged. The authors wish to thank Liang Guo and Dr. Jianli Wang for helpful discussions and assistance with the pulse shaping experiments.

[1]R. J. Ellingson, M. C. Beard, J. C. Johnson, P. Yu, O. I. Micic, A. J. Nozik, A. Shabaev, and A. L. Efros, Nano Lett. **5**, 865–871 (2005).
[2]M. C. Beard, A. G. Midgett, M. C. Hanna, J. M. Luther, B. K. Hughes, and A. J. Nozik, Nano Lett. **10**, 3019–3027 (2010).
[3]J. M. Luther, M. C. Beard, Q. Song, M. Law, R. J. Ellingson, and A. J. Nozik, Nano Lett. **7**, 1779–1784 (2007).
[4]L. A. Padilha, J. T. Stewart, R. L. Sandberg, W. K. Bae, W.-K. Koh, J. M. Pietryga, and V. I. Klimov, Acc. Chem. Res. **46**, 1261–1269 (2013).
[5]A. J. Nozik, Annu. Rev. Phys. Chem. **52**, 193–231 (2001).
[6]W. A. Tisdale, K. J. Williams, B. A. Timp, D. J. Norris, E. S. Aydil, and X.-Y. Zhu, Science **328**, 1543–1547 (2010).
[7]J. B. Sambur, T. Novet, and B. A. Parkinson, Science **330**, 63–66 (2010).
[8]Y. Yang, W. Rodríguez-Córdoba, X. Xiang, and T. Lian, Nano Lett. **12**, 303–309 (2012).
[9]B. T. Spann, S. V. Bhat, Q. Nian, K. M. Rickey, G. J. Cheng, X. Ruan, and X. Xu, Phys. Chem. Chem. Phys. **16**, 10669–10678 (2014).
[10]L. Brus, Appl. Phys. A: Mater. Sci. Process. **53**, 465–474 (1991).
[11]A. L. Efros, V. A. Kharchenko, and M. Rosen, Solid State Commun. **93**, 281–284 (1995).
[12]V. I. Klimov, Phys. Rev. Lett. **80**, 4028–4031 (1998).
[13]V. I. Klimov, Science **290**, 314–317 (2000).
[14]P. Kambhampati, J. Phys. Chem. C **115**, 22089–22109 (2011).
[15]B. T. Spann, L. Chen, X. Ruan, and X. Xu, Opt. Express **21**, A15–A22 (2013).
[16]B. T. Spann and X. Xu, J. Phys. Chem. C **118**, 2844–2850 (2014).
[17]J. L. Machol, F. W. Wise, R. C. Patel, and D. B. Tanner, Phys. Rev. B **48**, 2819–2822 (1993).
[18]A. Bragas, C. Aku-Leh, S. Costantino, A. Ingale, J. Zhao, and R. Merlin, Phys. Rev. B **69**, 205306 (2004).
[19]A. Bragas, C. Aku-Leh, and R. Merlin, Phys. Rev. B **73**, 125305 (2006).
[20]D. Sagar, R. Cooney, S. Sewall, E. Dias, M. Barsan, I. Butler, and P. Kambhampati, Phys. Rev. B **77**, 235321 (2008).
[21]Z. Chai, W. Wu, D. Kong, Y. Gao, and Q. Chang, J. Non-Cryst. Solids **382**, 121–124 (2013).
[22]G. A. Garrett, T. F. Albrecht, J. F. Whitaker, and R. Merlin, Phys. Rev. Lett. **77**, 3661–3664 (1996).
[23]T. Stevens, J. Kuhl, and R. Merlin, Phys. Rev. B **65**, 144304 (2002).
[24]Y. Wang, L. Guo, X. Xu, J. Pierce, and R. Venkatasubramanian, Phys. Rev. B **88**, 064307 (2013).
[25]A. Q. Wu and X. Xu, Appl. Phys. Lett. **90**, 251111 (2007).
[26]Z. C. Feng, P. Becla, L. S. Kim, S. Perkowitz, Y. P. Feng, H. C. Poon, K. P. Williams, and G. D. Pitt, J. Cryst. Growth **138**, 239–243 (1994).
[27]D. C. Hannah, K. E. Brown, R. M. Young, M. R. Wasielewski, G. C. Schatz, D. T. Co, and R. D. Schaller, Phys. Rev. Lett. **111**, 107401 (2013).
[28]J. Mooney, M. M. Krause, and P. Kambhampati, J. Phys. Chem. C **118**, 7730–7739 (2014).
[29]Y. P. Varshni, Physica **34**, 149–154 (1967).
[30]O. Madelung, *Semiconductors: Data Handbook* (Springer, 2004), pp. 815–835.